Transport and variability of the Antarctic Circumpolar Current south of Africa

[1]Sebastiaan Swart, [2]Sabrina Speich, [1]Isabelle Ansorge, [3]Gustavo Goni, [4]Sergey Gladyshev, [1]Johann R. E. Lutjeharms

[1]Department of Oceanography, University of Cape Town, Rondebosch, 7701, South Africa

[2]Laboratoire de Physique des Oceans, IFREMER, Universite de Bretange Occidentale, Brest, France

[3]Atlantic Oceanographic and Marine Laboratory, Physical Oceanography Division, NOAA, Miami, Florida, USA

[4]Shirshov Institute of Oceanology of Russian Academy of Sciences, 36 Nakhimovskii Prospect, Moscow, 117997, Russia

Abstract

Data from 21 hydrographic sections are used to estimate the baroclinic transport of the ACC south of Africa. Surface dynamic height (referenced to 2500 dbar) is derived from XBT data, by establishing an empirical relationship between vertically-integrated temperature and surface dynamic height calculated from CTD data. This temperature-derived dynamic height data compares closely (average RMS difference = 0.05 dyn m) with dynamic heights calculated from CTD data. A second empirical relationship between surface dynamic height and cumulative baroclinic transport has been defined allowing to monitor a more extensive time series of baroclinic transport, derived from upper ocean temperature sections. From 18 XBT transects of the ACC, completed south of Africa, the average baroclinic transport is estimated at 87.5 $\pm$ 3.97 Sv relative to 2500 dbar. This estimate is analogous with baroclinic transport values calculated from CTD data. Weekly maps of mean dynamic height (MDH) are used to deduce ACC baroclinic transport estimates by exploiting the relation between dynamic height and cumulative transport. The estimated mean baroclinic transport of the ACC, obtained this way, is 110 $\pm$ 18 Sv. These transports agree well with simultaneous in-situ estimates (RMS difference in net transport = 5.2 Sv). This suggests that sea level anomalies largely reflect baroclinic transport changes above 2500 dbar.

Improved measurements of baroclinic transport, using high density XBT sections, allow us to monitor the variability of the ACC's flow on improved spatial scales while altimeter derived baroclinic transports advance the temporal resolution, than could not be undertaken using previous methods.

1 Introduction

The Southern Ocean plays a unique role in coupling the ocean to the atmosphere and cryosphere. Southern Ocean dynamics are dominated by the extensive zonal flow associated with the Antarctic Circumpolar Current (ACC), which is the primary current that links all three ocean basins. The ACC is by far the largest conduit for the exchange of heat and salts between the subtropics and the higher latitudes as well as between the Atlantic, Indian and Pacific Oceans. These exchanges provide a vital mechanism by which the efficacy of the global overturning circulation is permitted, which in turn regulates the global climate system (Gordon, 1986; Rintoul, 1991; Speich et al., 2001). The interaction between the atmosphere, ocean and cryoshere in the Southern Ocean result in the creation for a number of water masses which ventilate the deeper layers and play an important role in the global thermohaline circulation (THC).

Polar-extrapolar communication of heat, freshwater and CO_2 provides a strong coupling between the ocean and atmosphere within the Subantarctic belt of the Southern Ocean, through the production of Antarctic Intermediate Water and Subantarctic Mode Water (McCartney, 1977; Piola and Georgi, 1982; Rintoul and England, 2002; Ansorge et al., 2004b). Baroclinic conditions associated with the upper thermal structure of the ACC are central to the meridional export of these water masses. These water masses spread northwards injecting cool, low saline water into and along the base of the main thermocline. The upwelling of Circumpolar Deep Water south of the ACC provides a pathway in the transport of heat from below 2000 m and into the atmosphere and cryosphere.

To the south of Africa, the ACC is largely influenced by the oceanographic regimes that extend beyond its northern and southern borders. The Agulhas Current system to the north, is regarded as one of the strongest western boundary currents in the world, driving exchanges of water between the Indian and

Atlantic Oceans, that has important implications on the THC (Gordon, 1985; 1986). The influence of the Agulhas Retroflection and associated ring shedding in this region plays an important role in the determining the latitudinal extent of the STC, and, therefore, the northward domain of the ACC (Figure 1). South of the ACC, the Weddell Gyre constitutes the largest cyclonic circulation regime in the Southern Ocean. The role of the Weddell Gyre is vital through the entrainment and transport of heat and salt from the ACC to the Antarctic Continental shelves, where deep and bottom waters are produced (Orsi et al., 1993).

In spite of these central elements, suitable Southern Ocean observational coverage is severely limited by the logistic difficulty of sampling and scarse routine hydrographic observations. This results in a poor understanding of the physical and dynamical processes that control the variability of the ACC and its influence on the THC. The GoodHope project launched in early 2004 (http://www.ifremer.fr/lpo/speich/GOODHOPE/goodhope.htm; Ansorge et al., 2004a) aims to establish an intensive monitoring programme that will provide detailed information on the varying physical structure and volume flux of water masses of the ACC in the region south of Africa. A key component of GoodHope is the implementation of a high density, expendable bathythermograph (XBT) repeat line between Cape Town and Antarctica (referred to as AX25), which runs largely along the TP-JASON 1 altimeter ground-track, serving for ground truthing altimetry-derived sea-height anomaly data. Furthermore, the southern fraction of the GoodHope monitoring line (south of 50°S) has already been sampled for several years by moorings of the German WECCON project. To the north, the GoodHope monitoring line overlapped with the USA AST-TEX programme (Byrne et al., 2006; Witter, 2006), thus linking the Southern Ocean dataset with that collected in the Benguela region.

Sustained observations along the GoodHope cruise track provide the means to monitor the vertical thermal and salinity structure and variability of the ACC and its associated fronts south of Africa. Such intense monitoring has been underway in the Drake Passage (Sprintall et al., 1997) and south of Australia (Budillon and Rintoul, 2003) since the 1970s. A major objective of the GoodHope programme is to provide sound estimates of ACC transport and variability using both in-situ measurements and remote sensing techniques. Previously, the only ACC transport estimates in the region of the Greenwich Meridian came from Whitworth and Nowlin (1987) and Legeais et al. (2005). Using CTD casts from the AJAX expedition, Whitworth and Nowlin (1987) estimated the baroclinic transport of the ACC to be 162 Sv to the bottom. From three CTD sections occupied near the Greenwich Meridian the baroclinic transports average 144.6 Sv relative to the bottom and 88.9 Sv relative to 2500 dbar (Legeais et al., 2005). Legeais et al. (2005) use proxy methods to derive the baroclinic transport of the ACC from 14 XBT sections conducted near the Greenwich Meridian. The mean of these baroclinic transport estimates is 97.5 Sv realtive to 2500 dbar and range from 87.5 Sv to 109.6 Sv. In contrary to the study by Legeais et al. (2005), the empirical relationships demonstrated in this paper allow us to apply remotely sensed data to the proxy techniques, thereby enhancing the spatial and temporal sampling resolutions.

In this paper we establish empirical relationships whereby dynamic height and baroclinic transport of the ACC can be determined from upper ocean temperature alone. Studying the baroclinic transport of the ACC provides a valuable way to improve our understanding of the processes occuring in the Southern Ocean that may have a large influence on the THC and the climate for the region. It is essential that researchers better understand modifications in the flow of the ACC between the three choke points (Drake Passage, south of Australia

and south of Africa). This allows us to quantify the leakage that occurs in and out of the ACC during its course to link all three major ocean basins and the associated effects this has on the THC (Gordon, 1986).

Furthermore, this study aims to better understand the upper thermal variability of the ocean region south of Africa. This is achieved by monitoring the position of the Southern Ocean fronts and dynamic height of the ocean. Dynamic height data helps to improve our knowledge of the ACC dynamics, which lead to variations in the temperature and salinity fields in both the short and long term. These estimates are crucial to better understanding the changes in the density field and its associated transport. However, our understanding of how the ACC transport varies and identifying long term changes in the baroclinic flow of the ACC, are still incomplete. This is largely due to the lack of observations completed during the austral winter months and because measurements are completed at such a low temporal resolution. We attempt to resolve this observational void by presenting a complete time series of ACC baroclinic transport south of Africa, using satellite altimetry data.

The data used in this study are defined in Section 2. Section 3 describes the upper thermal structure and frontal variability between Africa and Antarctica primarily using XBT data. We call on proxy methods to derive dynamic height data from upper ocean temperatures alone. The detailed procedures and results are shown in Section 4. In Section 5 we utilise all the available dynamic height data in the study region to derive baroclinic transport estimates off the ACC south of Africa and then analyse the meridional distribution of these transports in Section 6. A summarised transport budget over the south Atlantic Basin is depicted in Section 7. Finally, in Section 8, we show that it is possible to exploit satellite altimetry data to estimate the baroclinic transport of the ACC using the proxy relationships described in Section 4 and 5.

2 Data

2.1 Conductivity-Temperature-Depth

We use data from six CTD sections completed in the South-East Atlantic between November 1983 and October 2005. The sections provide a good coverage of the seasonal variability expected in the South-East Atlantic region because they are occupied during all seasons (Table 1). Two of these transects consist of repeats of the GoodHope cruise track completed by the Shirshov Institude, aboard the RV Sergey Vavilov. The undertaking of two CTD occupations along the GoodHope line allow us to improve the accuracy of geostrophic and baroclinic transport estimates from those already made by Legeais et al. (2005). In total, we use data from 276 CTD casts (of which 232 stations lie within the ACC domain), which connect Cape Town to Antarctica primarily along the Greenwich Meridian (Figure 2). The AJAX and A21 transects have the coarsest spatial resolution, where stations are spaced approximately 100 km apart as opposed to a 75 and 88 km spacing between stations occupied by the A12 and SR2-WOCE sections, respectively. The GoodHope II CTD section has a mean spacing of 43 km while the station spacing for GoodHope IV is 56 km. In most cases, tighter station spacing is found over regions of steep dynamic or bottom topography. The closer spacing between the GoodHope CTD casts allow us to investigate the meanders and mesoscale features in the ACC region of lengthscales of at least 200 km. Details concerning the CTD calibration, station positions, bottle analysis, problems encountered, and sampling carried out on each cruise can be found in a series of technical reports (Schripps, 1985; Roether et al., 1990; Lemke, 1992).

Section	AJAX	A21	A12	SR2	GH2	GH4
Date	Jan. '84	Jan.-Mar. '90	May-Aug. '92	Jan.-Feb. '93	Nov. '04	Oct. '05
Ship	RV Knorr	RV Polarstern	RV Meteor	SA Agulhas	RV Vavilov	RV Vavilov
Institution	Texas A&M U.	U. Bremen	A.W.I.	U. Cape Town	Shirshov	Shirshov
C. Scientist	T. Whitworth	W. Roether	P. Lemke	M. I. Lucas	S. Gladyshev	S. Galdyshev

Table 1: Summary of the CTD sections used in this study

2.2 Expendable Bathythermograph (XBT)

The deployment of XBTs by research and merchant vessels, which frequent the Antarctic bases, provides an economical and rapid means to collect ocean temperature data. Devoid of this method, full depth Conductivity-Temperature-Depth (CTD) casts, current meter moorings or pressure inverted echo sounder (PIES) arrays are needed to better understand the volume transport through the widest of the three 'choke points' of the Southern Ocean (approximately 4000 km between Africa and Antarctica). This vast distance and lack of scientific resources to do research in this remote region make the task of monitoring the transport of the ACC south of Africa very challenging.

The XBT data, in part, originates from 13 sections completed close to the Greenwich Meridian (Figure 3), between 1989 and 2006, as part of German and Russian research cruises and one ferry service completed by the University of Cape Town. Apart from the August 1989 section, sampling always took place in the summer months, between November and March. In addition to this, five repeat high-density XBT sections have been completed since February 2004 between Cape Town and Antarctica, as part of the GoodHope programme. The ocean climatology is extremely well resolved by utilising XBTs deployed at high resolution, which in turn improves our understanding of the ACC ocean dynamics and the location of associated surface and subsurface fronts south of Africa. The GoodHope cruise track runs south-west from the continental slope off Cape Town and along the T/P-Jason 1 altimeter ground tracks. At approximately 52°S, the cruise track intersects the Greenwich Meridian at which it continues south until reaching the Antarctic continent.

During the GoodHope transects, XBTs were deployed to measure the upper ocean temperature optimally at intervals of 25 km, increasing the frequency to 15 km over the main frontal regions associated with the ACC. Most deployments

reached a maximum working depth of the Sippican Deep Blue XBT of about 780 m. The GoodHope and Alfred Wegner Institute (AWI) XBT transects are measured with a vertical resolution of 2 dbar while the section completed by the Antarctic Russian Institute (AARI) has a vertical resolution of 1 dbar. The 4000 km transect between Africa and Antarctica was on average completed within two weeks, with each section providing a roughly synoptic picture of the upper thermal layer in this region of the Southern Ocean.

Extensive quality control procedures have been applied to the XBT data by AOML/NOAA in the United States. Adjacent temperature profiles were compared with each other and to the Levitus climatology (Levitus, 2001) in the region. On rare occasions, data gaps were found when XBTs failed as a result of high winds and sea swell, which caused the running signal wire to blow against the hull of the ship, thereby damaging the insulation. Profiles were declared bad and discarded if they did not reach a minimum depth of 400 dbar. When feasible and if the temperature data recovered well, 'spikes' in the profile were removed and edited. Occasionally, a profile was 'filtered' when differences in temperature appeared as spikes in the profile. This was usually caused by electrical interference or grounding problems on the ship.

2.3 Mean Dynamic Topography

Satellite altimetry measurements of sea surface height are used to estimate baroclinic transport. The 'Mean Sea Level Anomaly (MSLA)' product from CLS/AVISO, a weekly sea surface height (SSH) anomaly map on a $1/3^\circ$ Mercator grid that incorporates T/P, Jason-1, ERS-1/2 and Envisat altimeters, was used in this work. These multi-mission gridded sea surface heights are referenced to a seven year (1993-1999) mean. For details on mapping methods and error corrections applied to these fields, please refer to Traon et al. (1998), Traon and

Ogor (1998) and Ducet et al. (2000).

3 Upper thermal structure and frontal variability south of Africa

South of Africa, the ACC flows between the South Atlantic and South Indian subtropical domains in the north and the eastern part of the Weddell Gyre in the south. Since the ACC is not bounded by natural continental barriers south of Africa, such as at Drake Passage, it is important to accurately define the northern and southern Southern Ocean fronts, which delimits the ACC from the subtropical and polar flow regimes. We locate the ACC boundaries and fronts on the CTD and XBT sections using the temperature criteria proposed by Orsi et al. (1995) and listed in Table 2. These temperature criteria correspond accurately with the frontal positions, determined using salinity criteria, from the CTD sections.

Table 2: Temperature criteria used to detect the ACC fronts, reproduced from Orsi et al. (1995). STC is the Subtropical Convergence, SAF the Subantarctic Front, APF the Antarctic Polar Front, SACCF the southern ACC Front, SB the Southern Boundary and θ is the potential temperature.

Front	Temperature criteria
STC	$10°C < \theta_{100m} < 12°C$
SAF	$\theta >$ 4-5°C at 400 m, farther north
APF	$\theta < 2°C$ along θ_{min} at z $<$ 200 m, farther south
SACCF	$\theta > 1.8°C$ along θ_{max} at z $>$ 500 m, farther north
	$\theta < 0°C$ along θ_{min} at z $<$ 150 m, farther south
SB	Southern limit of vertical maximum of $\theta > 1.5°C$, ($\sim$200m)

A time sequence of six sections (five repeat GoodHope occupations and the Antarctica - Cape Town section) between 2004 and 2006, depicts the temporal and latitudinal variability of the upper ocean temperature structure in the Atlantic sector south of Africa (Figure 4). All sections were occupied during either

the austral spring or summer months and, therefore, do not illustrate features typical for austral fall and winter.

Whereas each of the meridional temperature sections indicates the general features one would expect to find in this region, the upper ocean thermal structure does not remain constant with time and exhibits important temporal variability. We compare the latitudinal positions of the Subtropical Convergence (STC), Subantarctic Front (SAF), Antarctic Polar Front (APF) and South ACC Front (SACCF) for the six transects (Figure 5). The February 2006 section does not follow the GoodHope cruise track and, therefore, some spatial differences occur. However, no considerable variability in the sea height field is observed for the latitudinal bands of the SAF and APF (between February 2004-2006), revealing that no considerable variability in the frontal positions is characterized by the zonal sampling difference between the two transects.

A warm core, anticyclonic feature is found between the STC and SAF during the January 2005 (Figure 4c) and December 2005 (Figure 4e) sections. The temperature sections where these features are located reveal a warming of the waters beyond 800 m with surface temperatures reaching as high as 19.0°C during both the January 2005 transect and 15.5°C during the December 2005 transect. The intense feature seen in the January 2005 section causes a strong meridional temperature gradient, where at 300 m the temperature increases from <8°C to >13°C over less than 60 km. The diameter of the warm core eddy is approxiamately 400 km at 200 m. Even though this constitutes a strong warm anomaly for this region, it does not necessarily affect the latitudinal position of the SAF, but rather it strengthens the temperature gradient across the front. On this occasion the position of the SAF was found to lie at 44.22°S. Due to the absence of warm or cold features in the remaining sections, a uniform horizontal temperature gradient is found between 41-44°S.

The sequence of frontal latitudinal positions, shown in Figure 5, reveals a southward shift in both the SAF and APF, at least during the spring and summer months. Between 2004-2006, the SAF moved 1.16° (130 km) southward while the APF shifted 2.65° (294 km) southward. Much of this signal would be induced by seasonal warming of the upper thermal layer as revealed by the southward shift in the fronts between early summer and late summer months. During the summer (winter) months these fronts are located to the south (north) of their mean annual locations. However, when the latitudinal positions of the SAF and APF for each February month are compared, a clear southward trend in these two fronts is evident. Even though the comparison is only made over two years, it may still suggest localised warming of the Southern Ocean in this region. Previously, Gille (2002) has analysed temperature data from Lagrangian floating platforms to show that the Southern Ocean, and in particular the ACC, has warmed by 0.17°C since the 1950s. This resulted in a southward shift of the ACC by approximately 50 km. More recently, a study by Cai (2006), has revealed that an observed positive wind stress curl trend (1978 and onward NCEP/NCAR reanalysis), induced by Antarctic ozone depletion, drives an intensifying, southward shifting Southern Ocean super-gyre circulation leading to a greater southward influx of warm water in all three oceans, and contributing to the greater rate of warming.

4 Dynamic Heights from XBT data

In many ocean regions, well-defined temperature-salinity (T-S) relationships exist allowing to infer the salinity corresponding to each temperature observation. Due to the connections of the Southern Ocean with the cryosphere (formation and melting of sea-ice) and the fact that warmer, saltier subtropical waters border it to the north, temperature and salinity profiles generally cool and freshen

to the south, and at some locations the relationship is multi-valued (one temperature corresponds with several salinity values). This means that the T-S curve cannot always be exploited to yield dynamic height values and, instead, an alternative method needs to be explored. However, when restricted to the ACC, the T-S curve is stable enough to estimate dynamic heights using temperature data alone.

Rintoul et al. (1997) have shown that a tight correlation exists between the average upper ocean temperature and dynamic height south of Australia. This relationship also exists in the ACC region south of Africa ($r = 0.95$, significant at the 95% level). This relationship proves to be extremely useful because XBT data, which extends to only 800 m, can then be used to derive dynamic heights at the surface. To test this relationship, several average temperature with pressure ranges were used: 100-200 dbar, 300-400 dbar, 600-700 dbar and 0-600 dbar. It was found that utilising the average temperature between 0-600 dbar was best suited to derive an empirical relationship with dynamic height at the surface (relative to 2500 dbar). Figure 6 shows the empirical relationship between temperature averaged between 0-600 dbar and dynamic height at the sea surface relative to 2500 dbar using data from the six CTD sections completed in the Atlantic sector south of Africa (Figure 2). Four of these CTD sections, AJAX, A21, A12 and SR2 (completed during February 1984, February 1990, May 1992, and January 1993, respectively) were used because they correspond spatially with the GoodHope transect while the remaining two CTD sections were occupied along the GoodHope line.

Although the CTD sections are from different seasons of different years, the data collapse onto a single curve, showing that this relationship is stable for this region of the Southern Ocean. The shape of the curve generally reflects the meridional variability of salinity from north to south. The larger scatter of

points, where temperatures exceed 7°C, is due to the influence of Agulhas Water north of the STC. This region has higher temperatures and salinities brought into the region by Agulhas Rings and filaments, which shed off the Agulhas Retroflection to the east. The drop in dynamic height below 3°C results in a steep gradient, which is caused primarily by the southward increase in upper ocean salinity (34.3 to 34.7) and drop in meridional ocean temperature between 49°S and 55°S. The mean dynamic height drop across the ACC for the six CTD sections is 1.1 ± 0.06 dyn m.

The mean ocean temperature between 0-600 dbar (T_{0-600}) from the 18 available XBT stations for the region are used to investigate their latitudinal dependence (Figure 7). The data points fall on a relatively tight curve over the domains of the ACC, but diverge to the north and south. The region to the north of the ACC (north of approximately 40°S) experiences a highly energetic field of anticyclonic and cyclonic eddies originating from the Agulhas Current and its Retroflection, which allows for exchanges of Atlantic, Indian and Southern Ocean water masses. The upper ocean thermal structure in this region is thereby variable, causing the upper ocean temperature range to spread significantly. The Southern Boundary marks the frontier separating waters flowing in the ACC from those found in the cyclonic sub polar Weddell Gyre. Poleward of the Southern Boundary, the upper ocean tends to have a greater range of temperatures due to the influence of diverse water masses (Park et al., 2001) associated with the transition between the ACC and the Weddell Gyre at roughly 56°S.

In order to estimate dynamic height from the available XBT sections, we exploit the empirical correlation shown in Figure 6 by applying a smoothing spline to the data. Fifth and eighth order polynomial fits were also tested and applied to the data. However, the smoothing spline provides a more accurate

method of interpolating values from this dataset. In recent years, it has been generally accepted (Emery and Thomson, 2001) that the smoothing spline is the most effective interpolation method. The smoothing spline is a particular non-parametric estimator of a function. Given a data set (xi, yi) it estimates values of y for y's other than those in the sample. Splines, unlike other polynomial interpolation formula, apply to a series of segments of the data record rather than the entire data series (Emery and Thomson, 2001).

To assess the ability of this method to infer dynamic height from XBT temperature data, we first compare the actual dynamic height relative to 2500 dbar to the estimates predicted by the regression relationship for the six available CTD transects. The actual CTD dynamic heights are withheld from the relationship when the empirically based dynamic heights are derived, in order to avoid bias. The results and corresponding root mean square difference (RMSD) over the ACC domain are shown in Figure 8. The mean of the RMSD for the six CTD sections is 0.05 dyn m. The agreement between the two estimates are excellent and the RMSDs are small. Discrepancies between the two estimates are largest near the northern and southern boundaries of the ACC, where the empirical relationship is less tight likely due to the mixing of different water masses found at the boundaries and where the spread of upper ocean temperature increases (as shown in Figure 7). Due to the higher resolution of the two CTD stations ($\sim$50 km), occupied along the GoodHope cruise track by the Shirshov Institute of Oceanology, mesoscale features are better resolved causing the dynamic height data to vary more than found in the remaining four CTD sections that have lower resolutions. The Southern Ocean fronts, especially the SAF and APF are well represented in the dynamic height gradients.

Dynamic heights are now estimated from the 13 XBT sections and five repeat GoodHope XBT transects using the empirical relationship. These estimates

have a marked latitudinal dependence, particularly within the ACC domain, and compare closely with true dynamic heights from the CTD sections (Figure 9). Once again, the values north of the STC and poleward of the Southern Boundary exhibit a large dispersion due to the large temperature range in upper ocean associated with these regions. Fortunately, for the purpose of this study, we focus specifically on the ACC, i.e. on the domain between the STC and the currents southern boundary, where the empirical relationship is particularly stable. Further, we illustrate the dynamic height estimates for the GoodHope repeat XBT transects in Figure 10. The mean net dynamic height drop from the northern to the southern boundary of the ACC for the five XBT sections is 1.1 $\pm$ 0.065 dyn m, which is the same as the mean CTD dynamic height drop off. The range of the dynamic height drop across the ACC is between 1.01 dyn m in February 2004 to 1.20 dyn m in November 2004. This indicates a range of 0.19 dyn m over the ACC. The three inner frontal positions are marked along the dynamic height profiles. Rapid decreases in the dynamic height are well produced over the SAF during the GH2 (November 2004) and GH3 (January 2005) transects. The dynamic height drop across the APF and SACCF is well reproduced during all the transects. This evidence shows that we can accurately determine the Southern Ocean frontal positions where large gradients in dynamic heights are encountered. This furthers the opportunity to determine the frontal positions using the gradients of sea height derived from satellite sea surface height.

5 Baroclinic transports from XBT data

In order to derive baroclinic transports of the ACC from temperature data alone, we derive a second empirical relationship between dynamic height, relative to 2500 dbar (DH_{2500}), and cumulative baroclinic transport, integrated northward

and above the 2500 dbar isobath (CT_{2500}) (Figure 11). This is prepared using data from five of the CTD transects completed in the South-East Atlantic. This method has been used to derive baroclinic transports from altimeter data for the region south of Australia (Rintoul et al., 2002). Similarly to Rintoul et al. (2002), we use here 2500 dbar as the reference level because it is the deepest depth that lies above the height of the mid-ocean ridge. There is a close relationship between the two variables ($r = 0.98$, significant at the 95% level), suggesting we can estimate baroclinic transports using dynamic height at the surface. We apply a smoothing spline to the data in order to estimate baroclinic transports derived from hydrographic dynamic height.

The accuracy of this method to infer baroclinic transports from upper ocean temperature is evaluated here. The dynamic heights for the CTD sections were computed using upper ocean temperature using the $T_{0-600} - DH_{2500}$ relationship and then applied to the $DH_{2500} - CT_{2500}$ relationship to derive baroclinic transports. These transports were then compared to baroclinic transport estimates derived from the five CTD sections relative to 2500 dbar. Resulting baroclinic transports and RMSDs are shown in Table 3 and Figure 12. The mean RMSD for the five tested sections is 6.0 Sv (1 Sv = 10^6 $m^3 s^{-1}$). This RMS error between baroclinic transports is relatively high, although, the end transports compare well. The mean baroclinic transport for the five sections is 87.9 $\pm$ 3.9 Sv compared with $DH_{2500} - CT_{2500}$ derived baroclinic transports which averaged 91.5 $\pm$ 1.2 Sv. On average, cumulative baroclinic transport values obtained from the $DH_{2500} - CT_{2500}$ relationship exceed CTD derived baroclinic transports by 3.6 Sv while the mean difference is 3.5 Sv, or only 4% higher.

We apply this proxy method to 18 XBT sections located in close proximity to the CTD transects. Several XBT sections are situated further eastward

Table 3: Comparison between baroclinic and temperature derived transports for five CTD sections. RMSDs are given over the entire section. All values are in Sv.

Section	CTD Baroclinic Tr	$DH_{2500} - CT_{2500}$ Tr	Difference	RMSD
AJAX	85.0	92.6	7.6	4.6
A21	89.1	90.4	1.3	4.5
A12	94.3	90.3	-4.0	8.8
GH2	86.2	91.1	4.9	6.1
GH4	85.0	92.8	7.8	6.0
Mean $\pm$ Std	87.9 $\pm$ 3.9	91.5 $\pm$ 1.2	3.5	6.0

of the CTD transects. These sections exhibit a poleward shift in the STC in this region causing the average northern ACC limit on the XBT lines to be displaced southward relative to the average value from the CTD transects (41.8°S versus 40.3°S) (Legeais et al., 2005). The XBT-inferred ACC baroclinic transports (above and relative to 2500 dbar; Tr_{2500}) range from 85.2 Sv to 94.7 Sv, with a mean of 90.0 $\pm$ 2.4 Sv (Table 4). This is only 2.1 Sv (or 2.3%) higher than the 87.9 $\pm$3.9 Sv average from the CTD sections. Figure 13, shows the baroclinic transport for the five repeat GoodHope sections and the Antarctica - Cape Town (AA-CT) section between February 2004 and February 2006. Differences in baroclinic transport at each station pair are represented by the stems. Increases in net baroclinic transport occur extensively over the major fronts of the ACC. The substantial increase and then decline in baroclinic transport near the northern end of the GH3 section is as a result of the intense Agulhas Eddy that was crossed. These baroclinic transport estimates are biased towards the summer months when sampling primarily occured.

There is no clear inter-annual pattern in net baroclinic transport. The net baroclinic transport does, however, tend to increase during the mid to late summer months when compared to sections completed in the early summer/spring months of the same season. The temperature sections show that the isotherm gradients steepen as seasonal progression warms the upper ocean layers. This

Table 4: Empirically derived baroclinic transports relative to 2500 dbar and the bottom, estimated for 18 XBT sections. Transports are given in Sv.

Section	Date	Tr_{2500}	Tr_{bottom}
viii2	Aug. 1989	92.9	150.0
viii3	Nov. 1989	91.2	147.3
ix3_1	Jan. 1991	87.8	141.9
ix3_2	Mar. 1991	90.9	146.8
x7	Dec. 1992	92.6	149.6
xii2	Nov. 1994	90.4	146.0
xii3	Jan. 1995	91.2	147.3
xv4	Mar. 1998	90.3	145.8
xvi2_1	Jan. 1999	87.1	140.6
xvi2_2	Mar. 1999	89.5	144.5
xviii3	Dec. 2000	90.5	146.1
AARI	Feb. 2004	94.7	152.9
GH1	Feb. 2004	87.9	142.0
GH2	Nov. 2004	89.9	145.2
GH3	Jan. 2005	90.9	146.8
GH4	Oct. 2005	85.2	137.5
GH5	Dec. 2005	86.2	139.2
AA-CT	Feb. 2006	90.9	146.7
Mean $\pm$ Std	-	90.0 $\pm$ 2.4	145.3 $\pm$ 3.9

increases the sheer in the dynamic height, which in turn intensifies the eastward baroclinic flow. The temperature at the southern end of the section is relatively constant with time, and, therefore, an increase in baroclinic transport tends to correspond to the presence of higher temperatures (and temperature gradients) in the northern domain of the ACC.

The average of the bottom referenced transport for four CTD sections is 145.0 $\pm$ 9.4 Sv. Due to the fact that CTD casts did not reach the bottom in the majority of the stations comprising the second CTD occupation of the GoodHope cruise track, no baroclinic transports relative to the bottom could be obtained for this section. The ratio between the baroclinic transport above 2500 dbar and to the bottom is almost constant and averages approximately 0.62 $\pm$

0.055. This ratio proves useful parameter to estimate the full depth baroclinic transports from XBT-inferred transports at 2500 dbar. When applying the 62% Tr_{2500}/Tr_{bottom} ratio, the bottom XBT-inferred ACC baroclinic transport ranges between 139 and 153 Sv, with a mean of 145 ± 3.9 Sv for the 18 XBT sections (Table 4).

6 Meridional baroclinic transport distribution

We now present results on the distribution of baroclinic transport over the meridional extent of the GoodHope section and examine the importance of hydrographic front dynamics to this distribution. The latitudinal distribution of the across section cumulated baroclinic transport for each repeat XBT section is shown in Figure 14. It is evident that throughout the sections there are anomalous periods of westward flow over short distance ranges. The most prominent of them are located at the northern end of the sections and are probably anticyclonic Agulhas warm core eddies crossed by the sections. This situation occurs during the first, third and fifth GoodHope transects, where proposed eddies are identified in the temperature sections (refer to Figure 4). The strongest of these is identified during the third GoodHope transect and produces large opposing baroclinic transports of 34 Sv westward at 41.5°S and 46 Sv eastward at 42°S. The magnitude of these transports suggests this feature is likely to be an Agulhas Ring, which has pervaded into the northern part of the ACC. The occurrence of similar features have been recorded by surface drifters and subsurface floats (at approximately 800 m depth) in the region of 41°S (Richardson, in press). In this study it was found that the Agulhas extension appears to split the South Atlantic Current (in the process, the northern ACC) into two branches and to transport Agulhas Water westward where it is eventually mixed and absorbed with eastward flowing water from the western Atlantic.

Weaker westerly flow is also found at the SAF and APF, where the baroclinic transport is expected to be more variable. The mean baroclinic transport, of five GoodHope XBT transects, has been divided into half degree latitudinal bands over the ACC domain (Figure 15a). Again, it is evident that the mean flow at the northern end of the section (north of 42°S) is found to have a surprisingly strong mean westward flow. The mean westward flow north of 42°S is calculated as 17.4 Sv. Two broad peaks of eastward baroclinic transport are found between the latitudinal ranges of the SAF and APF (arrow ranges in Figure 15). The local maximum in eastward flow at the 52.5°S band is associated with the SACCF. There is little mean additional eastward baroclinic transport (<1 Sv) south of the SACCF and at the Southern Boundary of the ACC.

The meridional distribution of variability in the baroclinic transport (Figure 15b) is highest in the region north of ∼42.5°S due to the east-west fluctuations in flow associated with the meandering STC and intruding Agulhas anticyclonic eddies. In this region, the standard deviation exceeds 12 Sv. Large standard deviations are also found over the SAF, Subantarctic Zone and APF and may reflect both meridional shifts in the frontal positions and changes in current strength. This was similarly shown to be the case along the SR3 and SURVOSTRAL sections completed south of Tasmania (Rintoul et al., 2002). South of 51°S, the variability is, as expected, substantially less (standard deviations less than 3 Sv), where the two southern most ACC fronts experience less seasonal warming and cooling associated with the changing seasons.

The baroclinic transports associated with the three inner ACC fronts, and their contribution to the net ACC baroclinic transport are calculated for each GoodHope transect and displayed in Table 5. This was done by accumulating the baroclinic transport between the point where the baroclinic transport was found to be zero or flowing westward to the south and to the north of the

Table 5: Mean position of the three inner ACC fronts and associated contribution of each front to the baroclinic transport of the ACC (in Sverdrups and percentage of net ACC baroclinic transport, relative to 2500 dbar)

Front	Mean Position (°S)	Transport (Sv)	% Transport of ACC
SAF	40.5 ±0.2	28.8 ±8.8	32.3 ±9.1
APF	44.6 ±0.5	24.8 ±7.4	28.4 ±9.0
SACCF	50.4 ±0.9	9.8 ±5.9	11.1 ±6.6
Total	-	63.4	72

axial front position. The XBT-inferred frontal contributions largely match those deduced from the CTD sections. The contribution from the SAF and SACCF for the XBT-inferred baroclinic transports were 5.4 and 4.5% less, respectively. An overwhelming fraction (72%) of the net ACC baroclinic transport is accounted for by the three inner ACC fronts of which the SAF and APF dominate with a 32% and 28% contribution, respectively. This emphasises the key role the fronts play in determining the total baroclinic transport of the ACC. Both the SAF and APF are primarily responsible for the variability associated with the total flow of the ACC. These two fronts have large baroclinic transport ranges which exceed 20 Sv (SAF: 21.7-42.9 Sv; APF: 15.9-34.4 Sv) and their standard deviations are 8.8 Sv and 7.4 Sv (or 9%), respectively.

7 ACC transports in the Atlantic sector

Measurements of transport in the Atlantic sector have dominated in the Drake Passage, where natural continental boundaries of the ACC simplify the computation of the total volume transport. Whitworth (1980) observed the baroclinic transport, relative to 2500 dbar, to average aproxiamately 80 Sv, while Nowlin and Clifford (1982) obtained a range of between 86-88 Sv referenced to the same level. More recently, Sokolov et al. (2004) calculated the baroclinic transport to be 92.7 Sv, relative to 2500 dbar from four CTD sections along the SR1

line, while upper ocean temperature derived baroclinic transports using proxy methods from these same data produced an estimate of 83.5 Sv. Our baroclinic transport estimates compare very closely with those of the Drake Passage. The mean geostrophic flow referenced to 2500 dbar, along or close to the Greenwich Meridian is 87.9 ±3.9 Sv, while the mean baroclinic transport estimates from the 18 XBT sections using the proxy method is 90.0 ±2.4 Sv. These results suggest that there is no net gain or loss in the ACC volume along the South Atlantic basin or from the South Atlantic Gyre when regarding the circulation in the upper 2500 dbar. One must keep in mind the uncertainties that may be created by temporal variations, and a barotropic transport contribution, when comparing the baroclinic transports along the longitudinal extent of the South Atlantic.

Between the Drake Passage and the Greenwich Meridian we find greater dynamical interaction between water masses associated with the ACC and those found to the north within the deeper level circulation (below the 2500 dbar isobar). There is substantial variations in the bottom referenced baroclinic transport between the Drake Passage, at 35°W, and at the Greenwich Meridian. Full depth mean baroclinic transports range between 134 ±11 Sv (Whitworth and Peterson, 1985) and 137 ±8 Sv (Cunningham et al., 2003; Sokolov et al., 2004) at the Drake Passage, while at 35°W, a study by Heywood and King (2002) found the baroclinic transport to be 157 Sv. Our full depth baroclinic transport estimate in the region of the Greenwich Meridian is 145 Sv from both the CTD baroclinic flow and from the 18 XBT baroclinic transport estimates, which is the same as the values obtained by Legeais et al. (2005). This result may consequently reveal that approximately 20 Sv are gained within the ACC between the Drake Passage and 35°W. This is ascribed to deep level injection of North Atlantic Deep Water (NADW) within the SAF in the western boundary

region, as shown through water mass breakdown proposed by Heywood and King (2002). This was previously proposed by Gordon (1986). In addition, Read and Pollard (1993) confirmed that there showed be some addition of NADW to the Circumpolar Deep Water (CDW) because of its higher salinity found further east at 40°E.

On the basis of isopycnal salinity distributions at deep levels (Arhan et al., 2003), it has been suggested that the decrease from 157 Sv at 35°W to 145 Sv at the Greenwich Meridian (net loss of 12 Sv), reflects a northward loss of CDW by the ACC (Legeais et al., 2005). If correct, this would be a partial compensation to the gain of NADW found to the west of 35°W, in the same depth range. Furthermore, the fact that transport estimates above 2500 dbar are similar between Drake Passage and the Greenwich Meridian supports the indication that net volume communication takes place at the deep levels. There may also be a loss of Lower CDW (LCDW) from the ACC to the Weddell Gyre between 35°W and the Greenwich Meridian. Evidence shows that most of the water warmer than 0.2°C in the Weddell Gyre is an unmodified remnant of LCDW from the southern ACC (Whitworth and Nowlin, 1987). This idea is supported by $\theta - O_2$ diagrams from the Criva-2 stations, which show a discontinuity in $\theta - O_2$ slopes between LCDW and AABW (Park et al., 2001).

Lastly, the bottom referenced baroclinic transport estimates of 157 Sv at 30°E (Legeais et al., 2005), of 157 Sv (Park et al., 2001) and of 159 Sv at 33°E (Read and Pollard, 1993) suggest that the ACC domain south of Africa gains between 9 to 14 Sv. Read and Pollard (1993) have suggested that this may be accounted for by a southward transfer of water across the STC south of the Agulhas Retroflection between 0 and 30°E. A summary of the ACC baroclinic transports in the Atlantic basin is shown in Figure 16.

8 Baroclinic transports inferred from satellite altimetry

A core aim of this paper is to show that baroclinic transport estimates of the ACC, at a substantially improved temporal resolution, can be undertaken. Hydrographic data are collected in the Southern Ocean primarily in the summer months and creates the risk of aliasing high frequency variability. Annual XBT and CTD transects are not frequent enough to resolve the net ACC baroclinic transport variability because annual sampling mostly reflects baroclinic transport variations in the mesoscale band. A continuous time series of mean dynamic height (MDH) is created by adding the altimeter sea level anomalies (multimission gridded sea surface heights product from AVISO; see Section 2.3) to the mean surface dynamic height relative to 2500 dbar calculated from two CTD and five XBT repeats of the GoodHope cruise track. The MDH reproduces the dynamic gradient accurately when compared to the CTD (Figure 17) and XBT dynamic heights. The MDH product is somewhat 'smoother' than the hydrographic dyanmic heights and in some cases mesoscale features are less well resolved. The hydrographic dynamic height estimates are relative to 2500 dbar and include only the baroclinic signal above this field. The altimeter derived MDH, however, may reflect changes in the density field transmitted to varying depths in the water column. Differences between the MDH and hydrographic dynamic heights, therefore, may in part originate from the baroclinic field below 2500 dbar, and the barotropic field. The differences may also reflect temporal and spatial sampling discrepancies, mapping errors and tides which have not been entirely removed from the altimeter signal, as well as errors incurred in attaining the CTD and XBT observations. Similarly, this was found to be the case when sea surface height anomalies, inferred from CTD and altimeter mea-

surements were compared south of Australia (Rintoul et al., 2002). Despite these factors, hydrographic estimates of dynamic height and the MDH are very similar (mean RMSD is 0.063 dyn m). This suggests that the MDH largely reflects baroclinic changes in the upper 2500 m of the water column.

Given that the ACC, south of Africa, is unbounded by any continental landmasses, it has an open ocean current structure. This becomes an advantage when estimating baroclinic transports using satellite altimetry products because no flow is ommited that occurs too close to coastal areas where altimeter data becomes unreliable due to tidal errors. This problem was encountered by Rintoul et al. (2002) south of Tasmania, where the flow between 45°S and the Tasmanian coast was excluded due to altimeter limitations. The northern and southern boundaries of the ACC are devised using a method by which the positions of the ACC fronts can be delineated using the MDH. The position of each front is determined by the local maximum in the MDH gradient in the relevant frontal regions (where one expects the isopycnals to be most inclined). The frontal positions estimated using this method compare closely with the in-situ infered locations from CTD and XBT sections, as determined using criteria by Orsi et al. (1995). The mean latitudinal difference in the position of the front using these two estimates is 0.22°, 0.09°, 0.01°, 1.07° and 0.16° for the STC, SAF, APF, SACCF and Southern Boundary, respectively.

We use the empirical relationship between dynamic height and cumulative baroclinic transport to estimate the baroclinic transport of the ACC (relative to 2500 dbar) from the MDH. To test this approach, we compare the baroclinic transport estimated from the MDH and from two CTD and five XBT occupations along the GoodHope track (Figure 18). Both the transports and the form of the two curves are well produced. The accretion of baroclinic transport over the SAF and APF is particularly well represented. The station pair differences

are generally less than 8 Sv but increase over sections that have a low station density. Sections with largely spaced stations cause more abrupt changes in the dynamic height over latitude (specifically the GoodHope 3 XBT section; Figure 18d). The mean RMSD between the two transport estimates is 7.1 Sv and 10.1 Sv for the CTD and XBT sections, respectively. Nearer the fronts (namely the SAF and APF), the MDH deduced baroclinic transport gradient is greater (i.e. greater transport increase over latitude). This may, in part, reflect the deep structure of fronts, which extend closer to the sea floor than the rest of the ACC regime, and which are responsible for a significant proportion of the ACC's net baroclinic transport (see Section 6). Other differences between the MDH and hydrographically derived baroclinic transports may be due to deep baroclinic flow (>2500 dbar), and mapping errors and tides, which have not been removed from the altimeter signal. An explanation for the difference between the two curves may be caused by the barotropic component of the flow captured in the altimeter signal and that is reproduced in the MDH product. If the effects of the deep baroclinic flow, mapping errors and tides are ignored, the residual transport derived from the MDH can be constituted as a barotropic transport estimate if we assume the dynamic height residuals in Figure 18 reflect the barotropic component of the MDH. In recent times, there has been slow progress made in determining the barotropic flow of the ACC. It is hoped that being able to measure the barotropic component of the ACC net transport, using satellite remote sensing techniques such as these presented here, will make a significant contribution to determining the absolute transport structure of the ACC.

9 Continuous time series of net ACC baroclinic transport

The MDH is used to estimate a 14 year continuous time series of net ACC baroclinic transport (Figure 19a) by exploiting the relationship between dynamic height and cumulative baroclinic transport (Figure 11). The baroclinic transports are integrated between the Southern Boundary of the ACC and the STC along the GoodHope track. The time series extends, at weekly intervals, between October, 14, 1992 and June, 7, 2006. The net baroclinic transport shows intense high frequency variability with a range of between 73-146 Sv and a mean of 109.5 Sv (standard deviation of 17.6 Sv). A linear trend shows that the net baroclinic transport has increased by 9.7 Sv over 14 years (or 6.9 Sv per decade).

The mean baroclinic transport between 1992 and 2000 is 105.6 Sv and subsequent to 2000 is 113.8 Sv, relating to a 8.2 Sv increase in baroclinic transport between the two periods. The net baroclinic transport does not exceed 120 Sv between the period July, 01, 1998 to the beginning of 2000. This is a period where the net baroclinic transport is at a minimum and the mean net transport is 99.9 $\pm$8.8 Sv.

10 Summary

The exploitation of data is extremely important in the Southern Ocean region, where it is especially hard to obtain due to its remoteness and harsh environment. In this study, we demonstrate how repeat CTD sections allow us to derive proxy techniques for determining the variability of the ACC using XBT and remote sensing data alone. These alternative methods are used to make frequent, accurate estimates of baroclinic transport with high spatial and temporal resolution.

First, we showed that a close correlation exists between upper ocean temperature and dynamic height. Surface dynamic heights were thereby derived from XBT profiles which demonstrated close comparison with 'true' dynamic heights calculated from CTD data. The agreement between the two estimates were excellent and differences were small (mean RMSD $<$0.05 dyn m). These differences were highest towards the southern and northern end of the sections, where communication between several water masses containing different temperature and salinity signatures was most extensive. The resulting dynamic heights showed close correspondence with the ACC fronts where local maxima in gradients were experienced as well as demonstrating accuracy at resolving mesoscale features evident in the temperature sections.

A similar empirical relationship between surface dynamic height and cumulative baroclinic transport was used to derive, with minimal error, the baroclinic transport from all available XBT dynamic height delineations. These transports were found only to be, on average, 2.3% higher than the actual geostrophic measurements. The ratio between 2500 dbar and bottom referenced CTD transports was relatively constant (67%), thereby allowing us to reference the XBT baroclinic transports to full depth. This permitted an ACC baroclinic transport budget between different longitudes across the South Atlantic basin of which the estimates were similar with those of previous works.

The mean distribution of baroclinic transport with latitude exhibited broad bands of eastward flow associated with the three inner ACC fronts. Expectedly, these fronts also contributed to extensive amounts of variability in the ACC flow. The most northern part of the sections displayed periods of extreme flow reversals contributing to the highest amounts of baroclinic transport variability. These occurrences were attributed to westward propagating Agulhas Rings which penetrated the northern domains of the ACC along the GoodHope tran-

sect. Similarly, this situation was revealed in surface drifters and subsurface (800 m) floats (Richardson, in press).

A MDH, over the ACC, was created by adding SSH anomaly data to a mean surface dynamic height. The MDH compared closely with dynamic heights from CTD and XBT data (mean RMSD of 0.063 dyn m). Similarly, we applied the MDH to the relationship between dynamic height and cumulative baroclinic transport to obtain a 14 year time series of net baroclinic transport estimates for the ACC south of Africa. This makes it possible to monitor the ACC baroclinic transport between Africa and Antarctica from space at a weekly resolution. The time series showed that there are intense high frequency pertubations in the ACC baroclinic transport and that a statistically insignificant increasing trend of 6.9 Sv per decade was evident since 1992.

As shown by Rintoul et al. (2002) and Sokolov et al. (2004), these proxy techniques were appreciably promising and justify added effort to refine them further. The progression of the GoodHope programme in coming years will improve these techniques through supplementary hydrographic sections and allow for precise transport estimates in the dynamic realm south of Africa. Future studies will likely see the exploitation of correlations to derive other properties of interest, such as heat and salt volume fluxes, which will provide invaluable information about important components of the THC. Also, these proxy techniques will hi-light the value remote sensing techniques have on monitoring the transport of the ACC and associated variability in a data sparse and abstracted region like the Southern Ocean. A study such as this, intends to abet refining instrumentation and techniques required for effective monitoring of the Southern Ocean environment.

Acknowledgements. The successful completion of the hydrographic surveys would not have been possible without the invaluable assistance of the captains,

officers, crew and scientists of the *S.A. Agulhas* and *Akademik Sergey Vavilov*. We are grateful to Silvia Garzoli and NOAA/OCO for their support to implement the XBT deployments in high density mode, to Molly Baringer and Qi Yao for their assistance in the quality control of the data at NOAA/AOML, and to Steven Cook, Robert Roddy, Craig Engler and Jim Farrington for their logistics support with XBT deployments. S. Swart especially thanks S. Speich for support during a total 5-month stay at the Laboratoire de Physique des Oceans, UBO, France and J.-F. Legeais for technical support. The work presented here is supported by the South African National Antarctic Programme (SANAP) and the Russian Academy of Sciences (Grant Meridian Plus #18.17.3) through the provision of funds and facilities. The authors also thank Dr A. Sokov for his effort in helping implement this programme and the Alfred Wegener Institute for Polar and Marine Research for the partial provision of data used in this study.

References

Ansorge, I. J., S. Speich, J. R. E. Lutjeharms, G. J. Goni, C. J. Rautenbach, W. Froneman, M. Rouault, and S. Garzoli. 2004a. "Monitoring the oceanic flow between Africa and Antarctica." *South African Journal of Science* 101:29–35.

Ansorge, I. J., S. Speich, C. J. W. Rautenbach, P. W. Froneman, and G. Goni. 2004b. "GoodHope I: Hydrographic, Biological and Meteorological Data Report." Tech. rep., University of Cape Town.

Arhan, M., H. Mercier, and Y.-H. Park. 2003. "On the deep water circulation of the eastern South Atlantic Ocean." *Deep Sea Res. Part I* 50:889–916.

Budillon, G. and S. R. Rintoul. 2003. "Fronts and upper ocean thermal variability south of New Zealand." *Antarctic Science* 15:141–152.

Byrne, D. A., D. L. Witter, D. R. Watts, N. R. Pettigrew, C. M. Duncombe Rae, and S. Baker-Yeboah. 2006. "Interocean Heat and Salt Transports from the Agulhas Leakage: First results from ASTTEX." *Eos Trans. AGU, Ocean Sci. Meet. Suppl.* 87(36):Abstract OS22C–03.

Cai, W. 2006. "Antarctic ozone depletion casues an intensification of the Southern Ocean super-gyre curculation." *Geophysical Res. Letters* 33(L03712).

Cunningham, S. A., S. G. Alderson, B. A. King, and M. A. Brandon. 2003. "Transport and variability of the Antarctic Circumpolar Current in Drake Passage." *Journal of Geophysical Research-Oceans* 108.

Ducet, N., P. Y. Le Traon, and G. Reverdin. 2000. "Global high-resolution mapping of ocean circulation from TOPEX/Poseidon and ERS-1 and-2." *Journal of Geophysical Research-Oceans* 105:19477–19498.

Emery, W. J. and R. E. Thomson. 2001. *Data analysis methods in physical oceanography.* Elsevier Science B. V., 2nd ed., pages: 281-285.

Gille, S. T. 2002. "Warming of the Southern Ocean since the 1950s." *Science* 295:1275–1277.

Gordon, A. L. 1985. "Indian-Atlantic Transfer of Thermocline Water at the Agulhas Retroflection." *Science* 227:1030–1033.

Gordon, A. L. 1986. "Inter-Ocean Exchange of Thermocline Water." *Journal of Geophysical Research-Oceans* 91:5037–5046.

Heywood, K. J. and B. A. King. 2002. "Water masses and baroclinic transports in the South Atlantic and Southern oceans." *J. Mar. Res.* 60:639–676.

Legeais, J. F., S. Speich, M. Arhan, I. J. Ansorge, E. Fahrbach, S. Garzoli, and A. Klepikov. 2005. "The baroclinic transport of the Antarctic Circumpolar Current south of Africa." *Geophysical Research Letters* 32.

Lemke, P. 1992. "WHP Cruise Summary Information: A12." Tech. rep., Alfred Wegner Institut fuer Polar und Meeresforschung, Bremerhaven, Germany.

Levitus, S. 2001. *World Ocean Atlas.* NOAA.

McCartney, M. S. 1977. "Subantarctic Mode Water." *Discovery Reports* pages 103–119.

Nowlin, W. D. and M. Clifford. 1982. "The kinematic and thermohaline zonation of the Antarctic Circumpolar Current at Drake Passage." *Journal of Marine Research* 40:481–507.

Orsi, A. H., W. D. Nowlin, and T. Whitworth. 1993. "On the Circulation and Stratification of the Weddell Gyre." *Deep-Sea Research Part I-Oceanographic Research Papers* 40:169–203.

Orsi, A. H., T. Whitworth, and W. D. Nowlin. 1995. "On the Meridional Extent and Fronts of the Antarctic Circumpolar Current." *Deep-Sea Research Part I-Oceanographic Research Papers* 42:641–673.

Park, Y. H., E. Charriaud, P. Craneguy, and A. Kartavtseff. 2001. "Fronts, transport, and Weddell Gyre at 30°E between Africa and Antarctica." *Journal of Geophysical Research-Oceans* 106:2857–2879.

Piola, A. R. and D. T. Georgi. 1982. "Circumpolar Properties of Antarctic Intermediate Water and Sub-Antarctic Mode Water." *Deep-Sea Research Part A-Oceanographic Research Papers* 29(6):687–711.

Read, J. F. and R. T. Pollard. 1993. "Structure and Transport of the Antarctic Circumpolar Current and Agulhas Return Current at 40°E." *Journal of Geophysical Research-Oceans* 98:12281–12295.

Richardson, P. L. in press. "Agulhas leakage into the Atlantic estimated with subsurface floats and surface drifters." .

Rintoul, S. R. 1991. "South-Atlantic Interbasin Exchange." *Journal of Geophysical Research-Oceans* 96:2675–2692.

Rintoul, S. R., J. R. Donguy, and D. H. Roemmich. 1997. "Seasonal evolution of upper ocean thermal structure between Tasmania and Antarctica." *Deep-Sea Research Part I-Oceanographic Research Papers* 44:1185–1202.

Rintoul, S. R. and M. H. England. 2002. "Ekman transport dominates air-sea fluxes in driving variability of Subantarctic Mode Water." *Journal of Physical Oceanography* 32:1308–1321.

Rintoul, S. R., S. Sokolov, and J. Church. 2002. "A 6 ye.ar record of baroclinic transport variability of the Antarctic Circumpolar Current at 140°E

from expendible bathythermograph and altimetry measurements." *Journal of Geophysical Research-Oceans* 107.

Roether, W., M. Samthein, T. J. Muller, W. Nellen, and D. Sahrhage. 1990. "Sudatlantik-Zircumpolarstom, Reise Nr. 11, 3 Oktober 1989-11 Marz 1990, Meteor-Ber. 90-2." Tech. rep., University Hmaburg, Hamburg, Germany.

Schripps. 1985. "Cruise Report: AJAX." Tech. rep., Schripps Institution of Oceanography/Texas AM University, USA.

Sokolov, S., B. A. King, S. R. Rintoul, and R. L. Rojas. 2004. "Upper ocean temperature and the baroclinic transport stream function relationship in Drake Passage." *J. Geophys. Res.* 109(C05001):doi:10.1029/2003JC002010.

Speich, S., B. Blanke, and G. Madec. 2001. "Warm and cold water routes of an OGCM thermohaline conveyor belt." *Geophysical Research Letters* 28:311–314.

Sprintall, J., R. Peterson, and R. Roemmich. 1997. "High resolution XBT/CTD measurements across Drake Passage." *WOCE Newsletters* 29:18–20.

Traon, P. Le, P. F. Nadal, and N. Ducet. 1998. "An improved mapping method of multisatellite altimeter data." *Journal of Atmospheric and Oceanic Technology* 15:522–534.

Traon, P. Y. Le and F. Ogor. 1998. "ERS-1/2 orbit improvement using TOPEX/POSEIDON: The 2cm challenge." *Journal of Geophysical Research-Oceans* 103:8045–8057.

Whitworth, T. 1980. "Zonation and Geostrophic Flow of the Antarctic Circumpolar Current at Drake Passage." *Deep-Sea Research Part A-Oceanographic Research Papers* 27:497–507.

Whitworth, T. and W. D. Nowlin. 1987. "Water Masses and Currents of the Southern-Ocean at the Greenwich Meridian." *Journal of Geophysical Research-Oceans* 92:6462–6476.

Whitworth, T. and R. G. Peterson. 1985. "Volume Transport of the Antarctic Circumpolar Current from Bottom Pressure Measurements." *Journal of Physical Oceanography* 15:810–816.

Witter, D. L. 2006. "Satellite Altimeter Observations of Regional Circulation during the Agulhas-South Atlantic Thermohaline Transport Experiment (ASTTEX)." *Eos Trans. AGU, Ocean Sci. Meet. Suppl.* 87(36):Abstract OS22C–04.

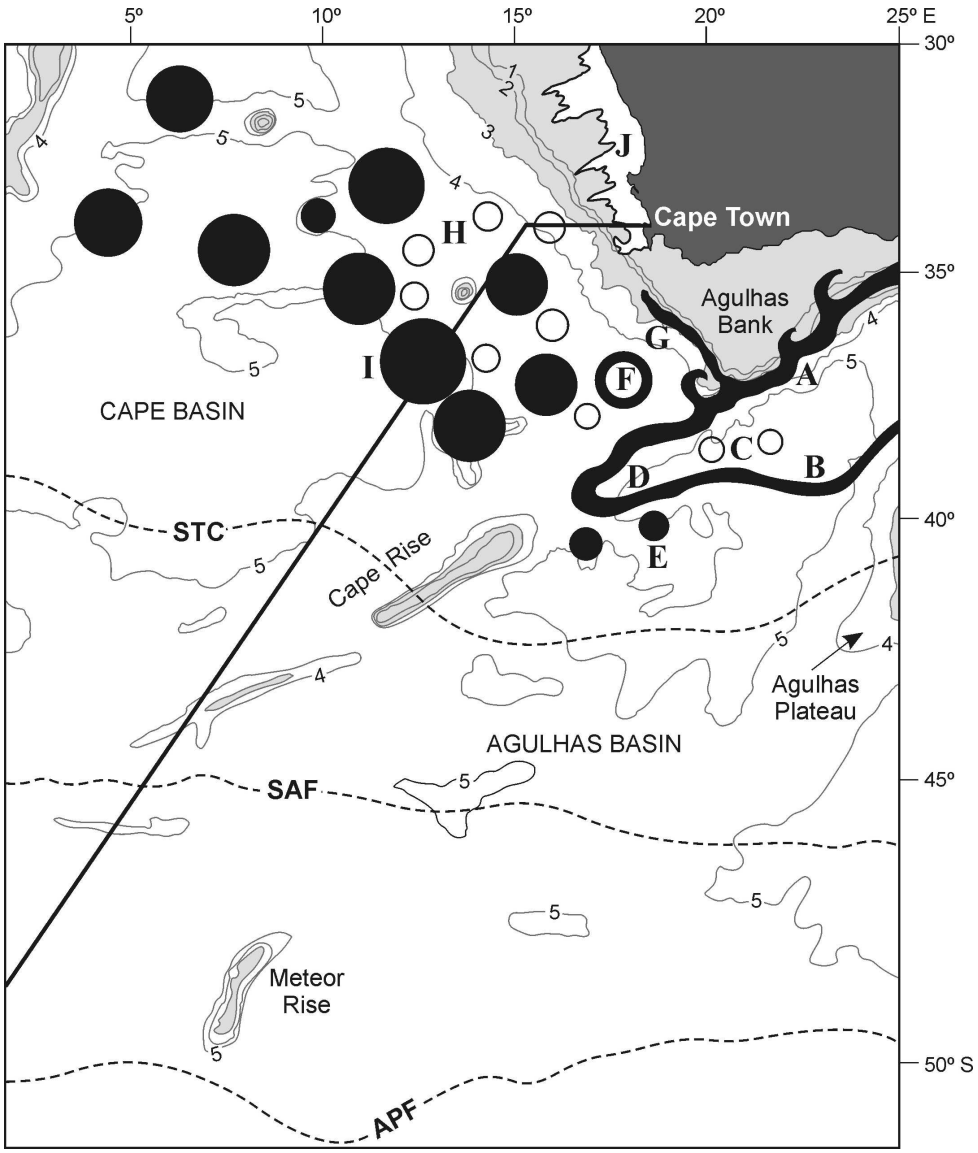

Figure 1: A conceptual diagram of the southern Agulhas Current system. Agulhas Rings (I) and filaments (G) are shed at the Agulhas Retroflection (D) and are carried equatorward by the Benguela Current (H). The Agulhas Current retroflects forming an eastward flow (B) to the north of the Subtropical Convergence (STC). The GoodHope transect (solid line) crosses the southern domains of the Benguela upwelling regime (J). The STC, SAF and APF denote the mean locations of the Subtropical Convergence, Subantarctic and Antarctic Polar fronts, respectively. Bathymetry contours are in km and depths less than 300 m are shaded.

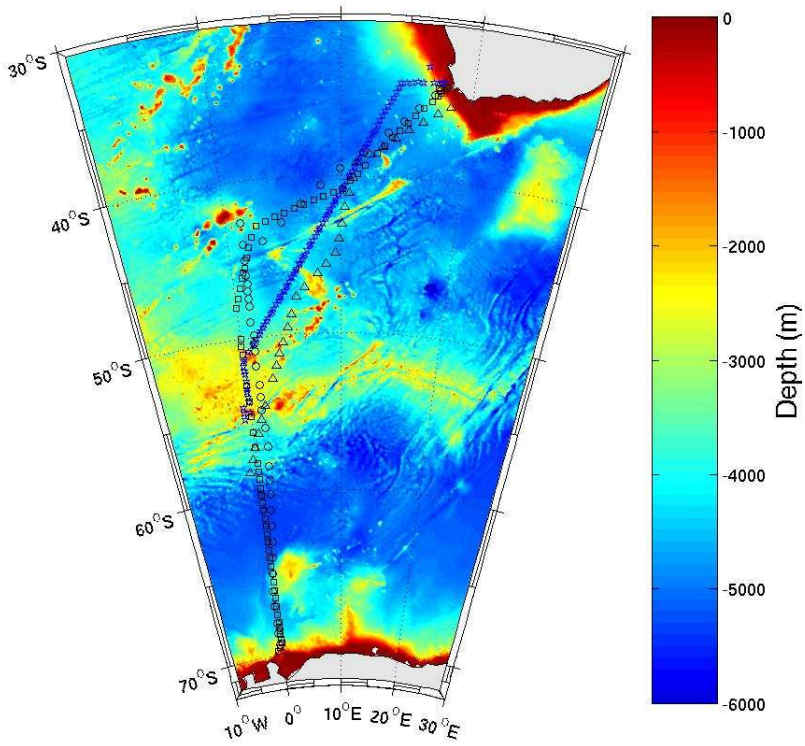

Figure 2: Locations of the six CTD sections used in this study (Table 1). The AJAX section (circles), A21 section (triangles), A12 section (squares), SR2 (diamonds), GoodHope 1 and 2 (stars). Bathymetry in meters below sea-level has been overlaid onto the section tracks.

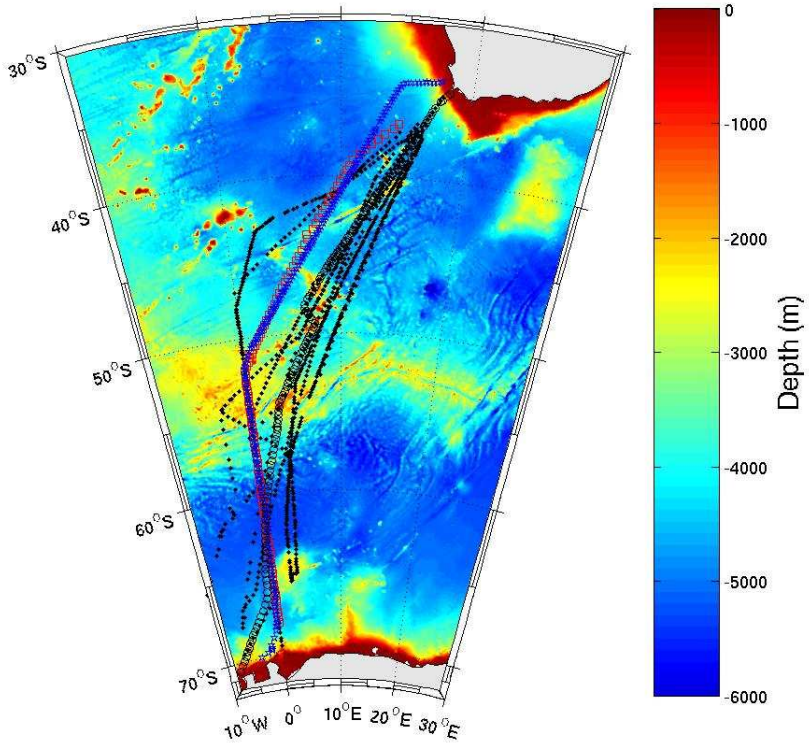

Figure 3: Locations of the XBT stations used in this study. GoodHope repeat section (stars), AARI section (squares), AWI sections (dots) and the AA-CT section (circles). Bathymetry in meters below sea-level has been overlaid onto the section tracks.

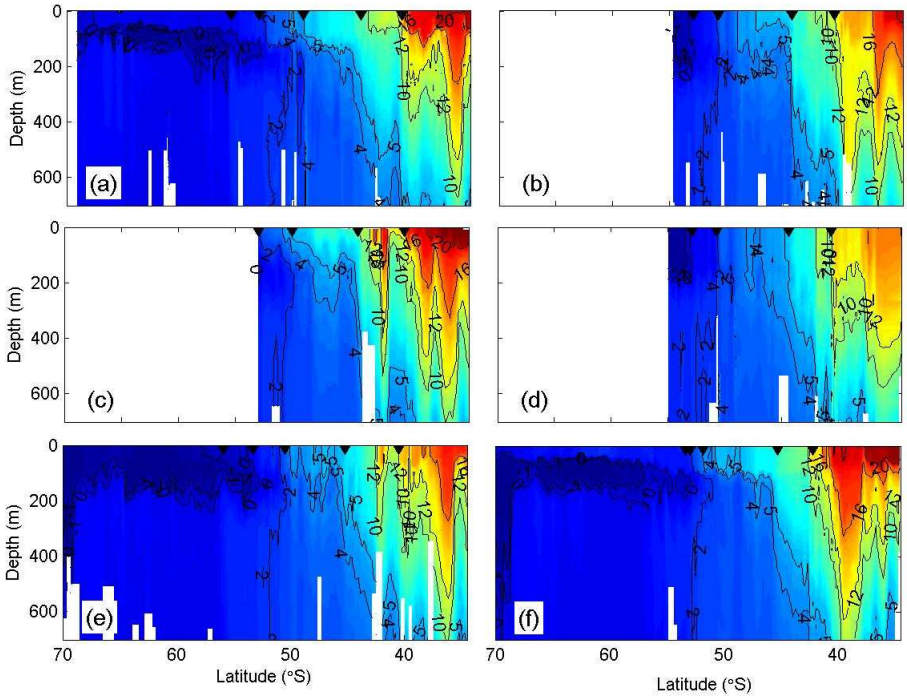

Figure 4: Temperature sections for five occupations of GoodHope and a transect between Africa and Antarctica between 2004-2006. (a) GoodHope I: February 2004, (b) GoodHope II: November 2004, (c) GoodHope III: January 2005, (d) GoodHope IV: October 2005, (e) GoodHope V: December 2005, (f) Antarctica - Cape Town (AA-CT): February 2006. The following isotherms are shown: -1, 0, 2, 4, 5, 10, 12°C. The black arrows show the latitudinal position of the ACC fronts (from south to north: STC, SAF, APF, SACCF, Southern Boundary). Triangles indicate station positions. Note that the figures have equal axes of depth and latitude.

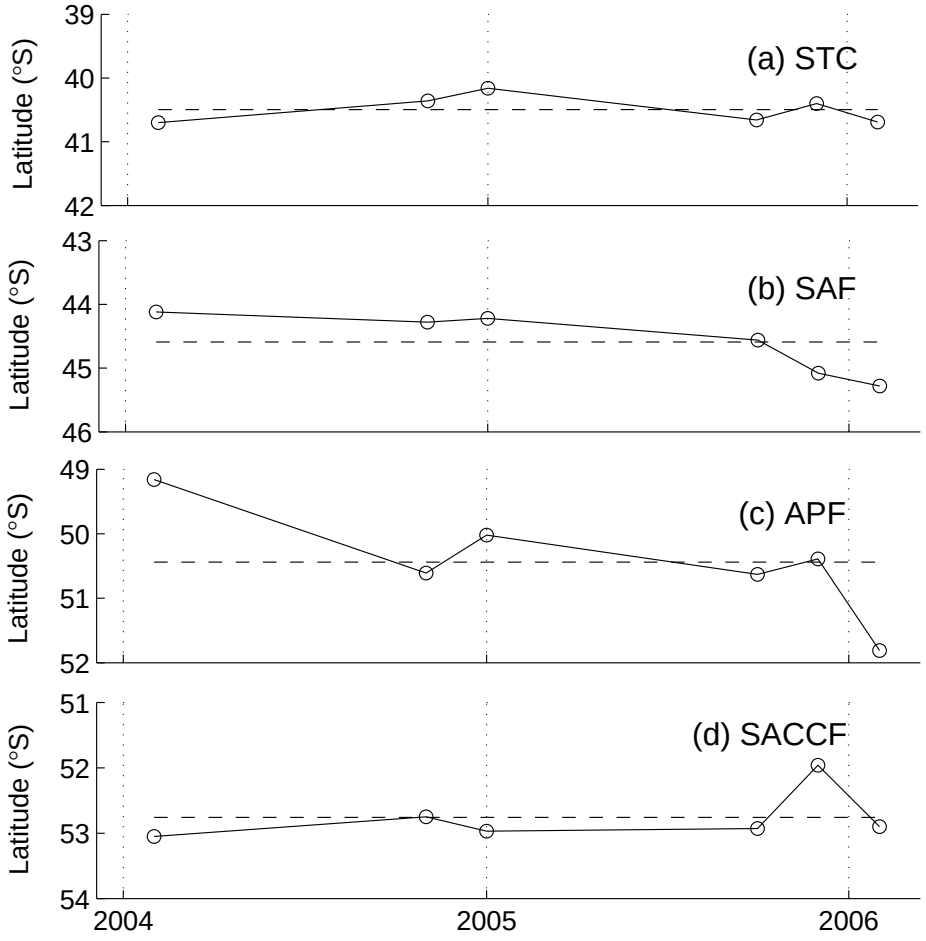

Figure 5: Latitudinal positions of the (a) STC, (b) SAF, (c) APF, (d) SACCF for the Africa to Antarctica transects completed between 2004-2006. The dashed line depicts the mean frontal position for six transects. Values of latitude are in °S.

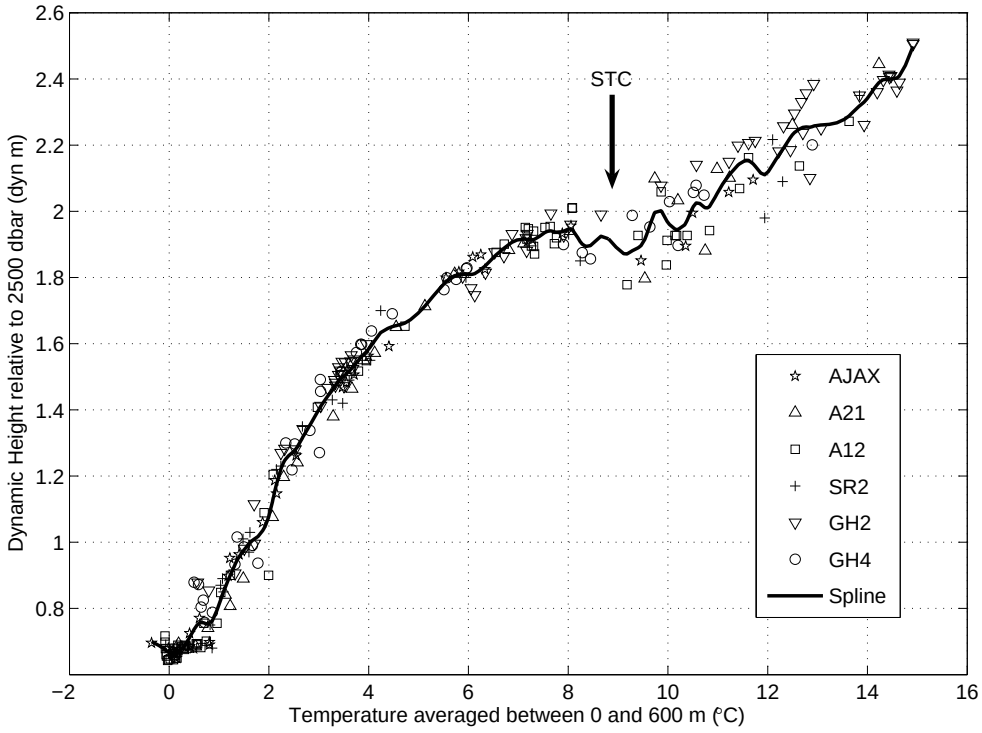

Figure 6: Dynamic height at the surface relative to 2500 dbar versus temperature averaged between the surface and 600 dbar. Data comes from six CTD transects completed in the south Atlantic: AJAX (stars), A21 (triangles), A12 (squares), SR2 (crosses), GH2 (down triangles), GH4 (circles). The solid curve depicts a smoothing spline fit to the data.

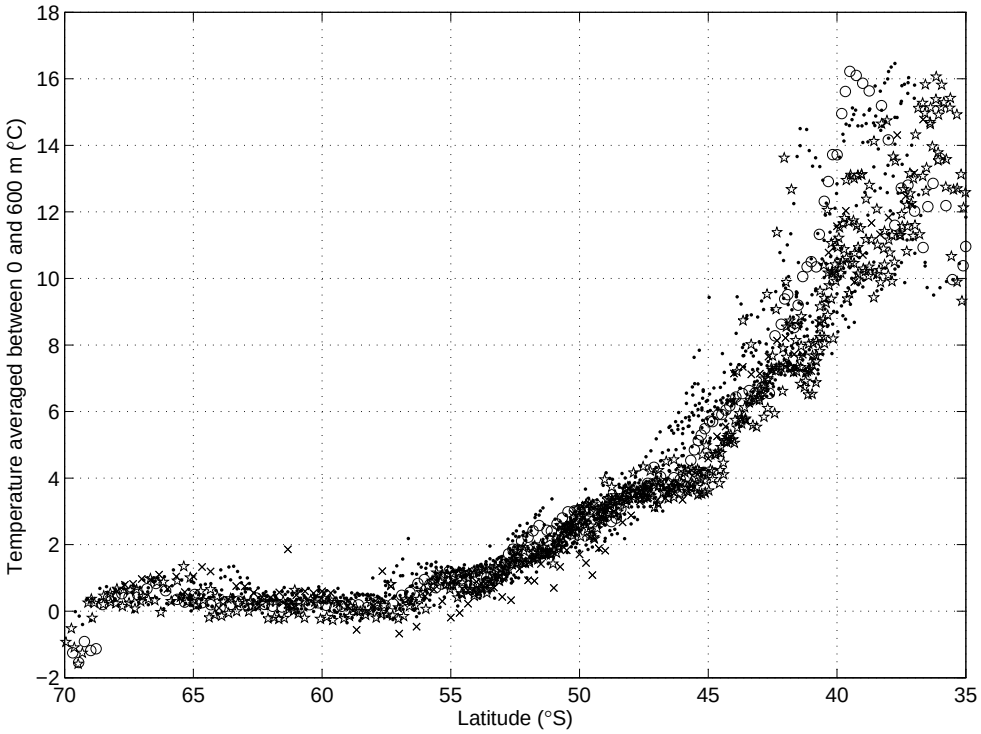

Figure 7: Average temperature between 0 and 600 dbar versus latitude for 18 XBT sections completed in the southeast Atlantic. Data comes from repeat GoodHope sections (stars), AA-CT section (circles), AWI sections (dots) and an AARI section (crosses).

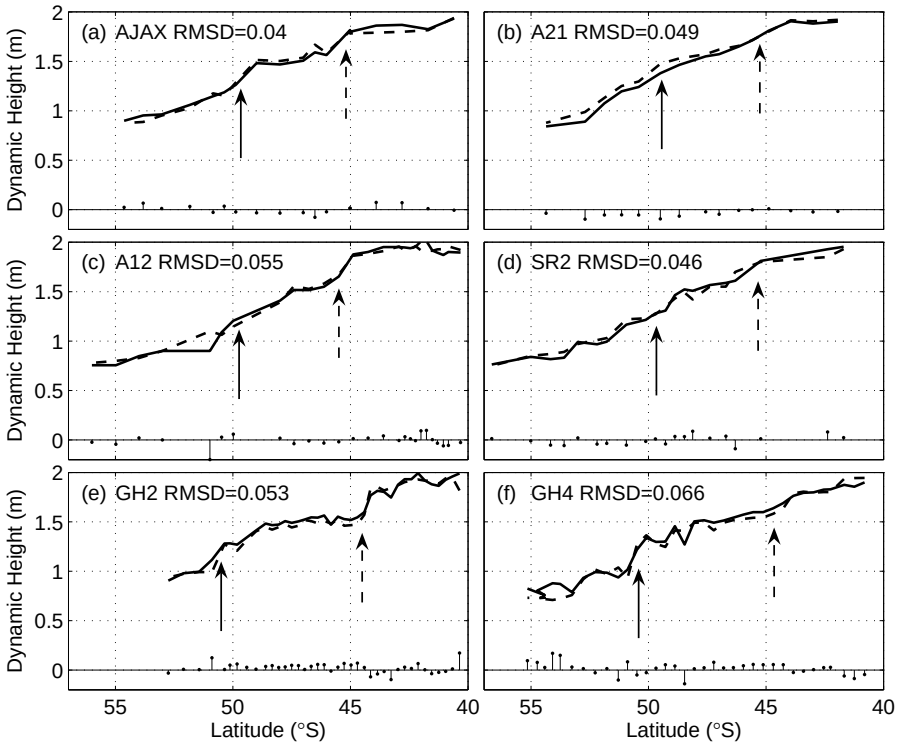

Figure 8: Comparison of 'true' dynamic height above 2500 dbar (solid line) and dynamic height derived from the empirical relationship (dashed line) between upper ocean temperature and dynamic height in Figure 6. The comparisons are made from each of the six CTD sections from which the data from the relevant section is withheld from the empirical relationship for each of these comparisons. The dashed and solid arrows represent the positions of the SAF and APF, respectively. Differences between the two dynamic heights are shown along the x axis. The RMSDs are given in dyn m.

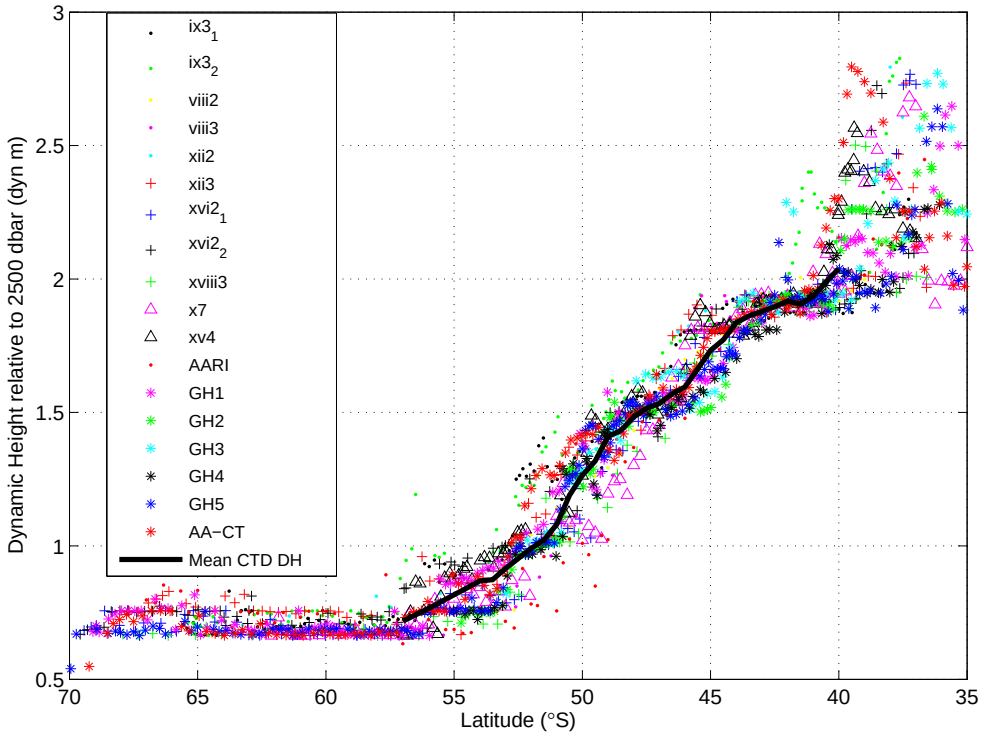

Figure 9: Dynamic height at the surface relative to 2500 dbar calculated using the regression relationship in Figure 6 versus latitude for 18 XBT sections. The solid line represents the mean dynamic height calculated from temperature and salinity data from the six CTD transects.

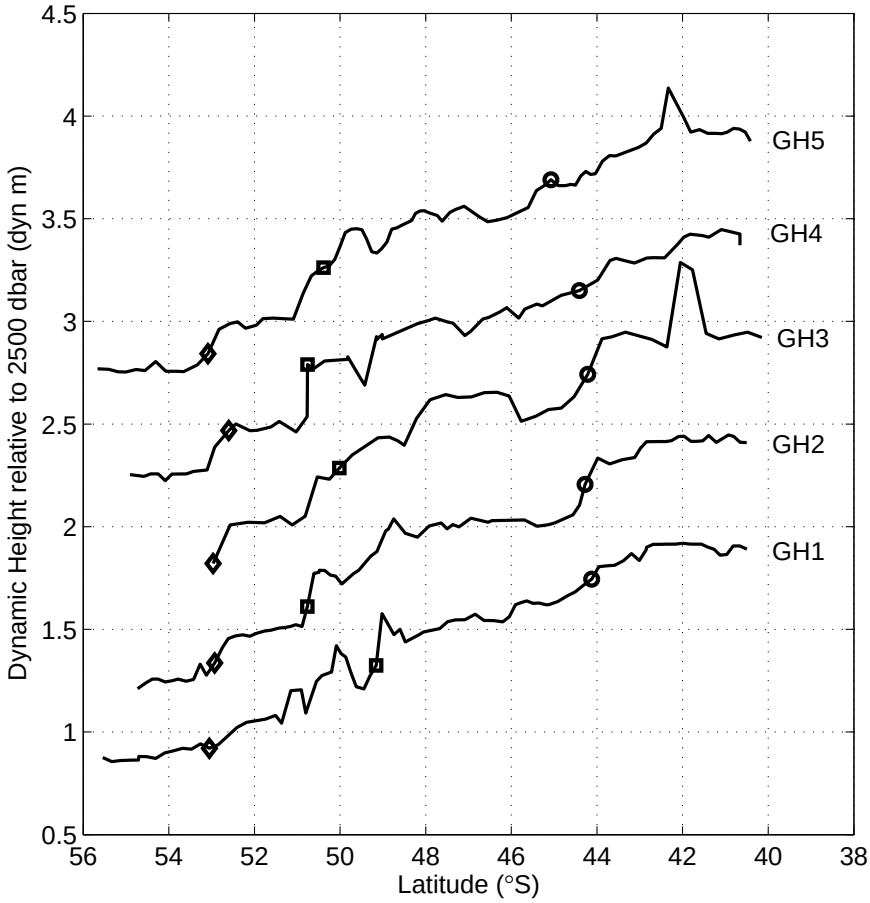

Figure 10: Dynamic height at the surface referenced to 2500 dbar for five repeat GoodHope XBT sections (2004-2006) estimated using the regression relationship in Figure 6. The estimated dynamic heights between sections are offset by 0.5 dyn m for clarity. The offset begins from the first section (GH1). The markers along each profile represent the latitudinal positions (found using the temperature sections) of the SAF (circles), APF (squares) and the SACCF (diamonds).

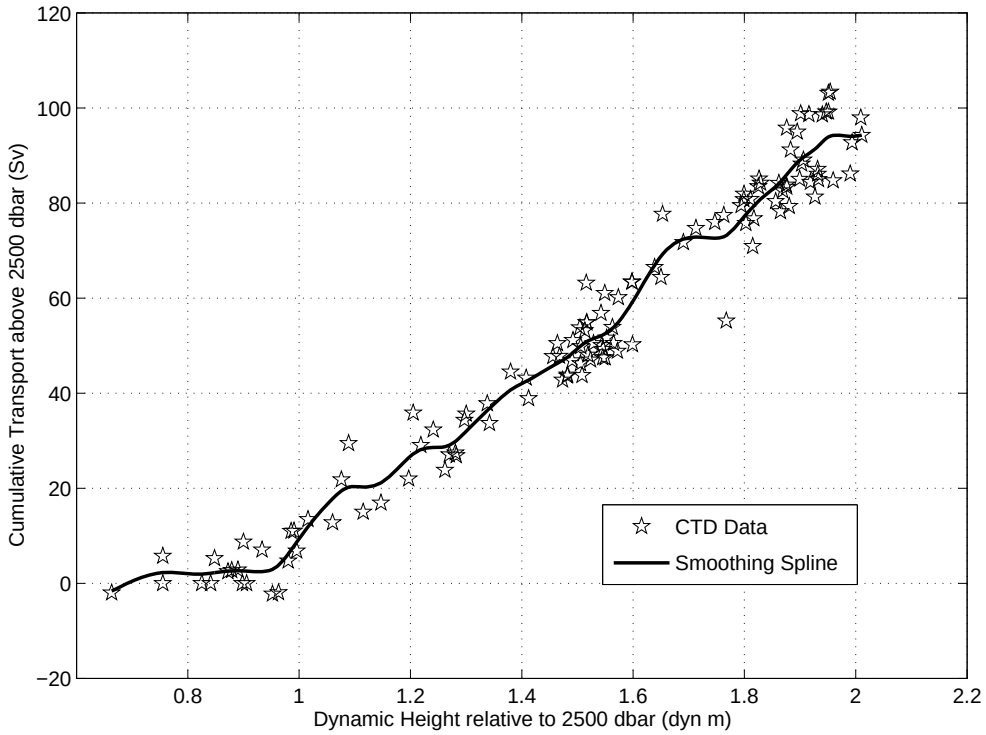

Figure 11: Northward cumulative transport (above and relative to 2500 dbar) versus dynamic height at the sea surface relative to 2500 dbar from five CTD transects completed in the South-East Atlantic (including two occupations of GoodHope). The solid curve depicts a smoothing spline fit to the data.

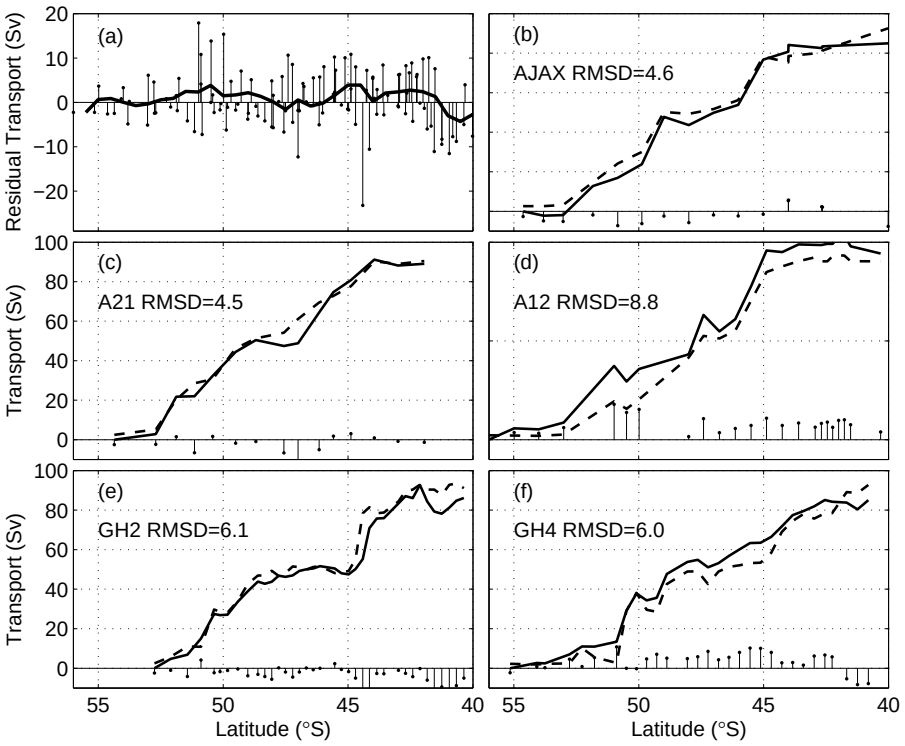

Figure 12: Comparison of geostrophic transport relative to 2500 dbar (solid line) and cumulative transport derived from the empirical relationship (dashed line) between dynamic height and cumulative transport in Figure 11. The comparisons are made from of five CTD sections. Differences between the two transports are shown along the x axis. The RMSDs are given in Sv. The differences between the curves are summarised in (a) and the solid line shows the mean residual plotted as a function of latitude.

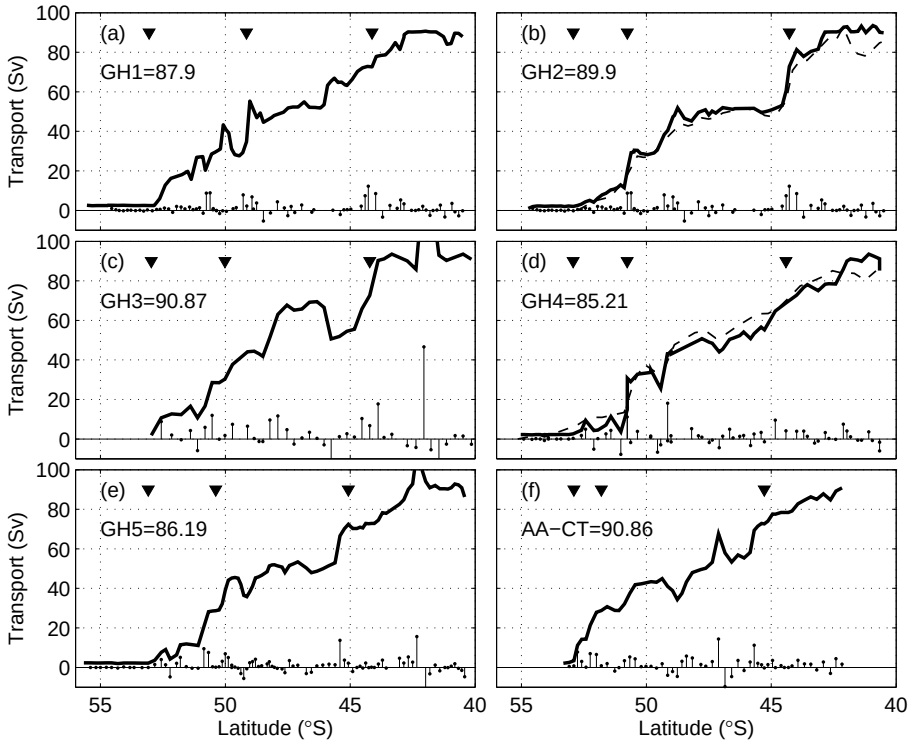

Figure 13: Northward cumulated baroclinic transport (referenced to 2500 dbar) for five repeat GoodHope XBT transects and the AA-CT section (bold line). The equivalent geostrophic transports from the CTD sections are shown for GoodHope 2 and 4 (dashed line). Differences in transport at each station pair are shown along the x axis. Values are given in Sv. The positions of the three inner fronts, determined from the temperature sections, are represented by the arrows (from south to north: SACCF, APF, SAF).

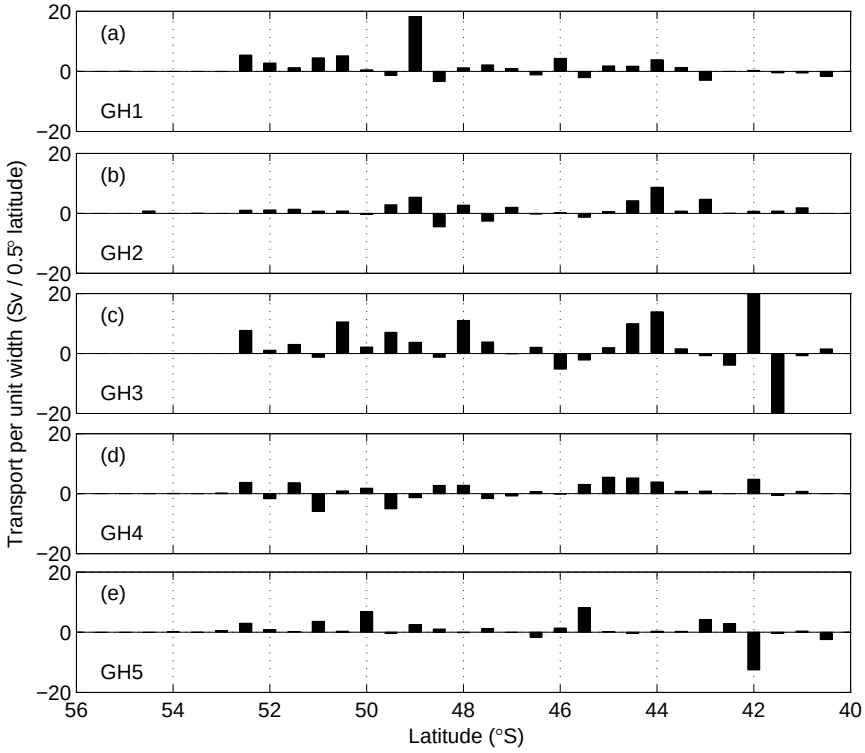

Figure 14: Baroclinic transport across the GoodHope sections per half degree latitude for five repeat occupations of GoodHope. Eastward flow is positive.

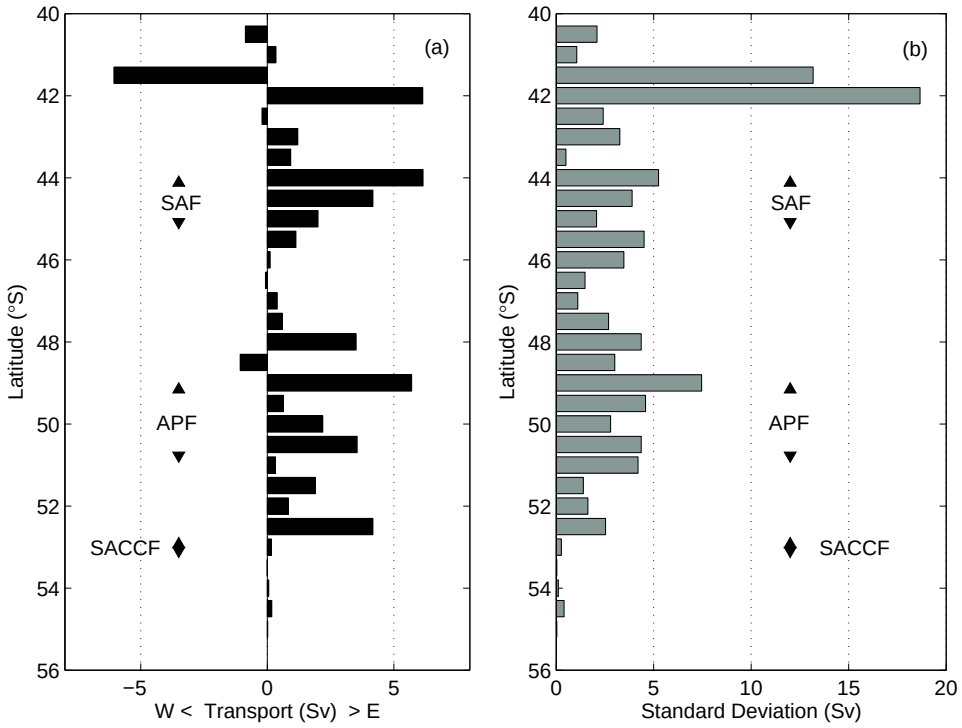

Figure 15: (a) Mean baroclinic transport, relative to 2500 dbar, per half degree latitude for five occupations of GoodHope. Eastward flow is positive. (b) The standard deviation of cumulative transport for the half degree latitude bands is given. The arrows indicate the latitudianl range of the three inner hydrographic fronts during the five repeat GoodHope occupations.

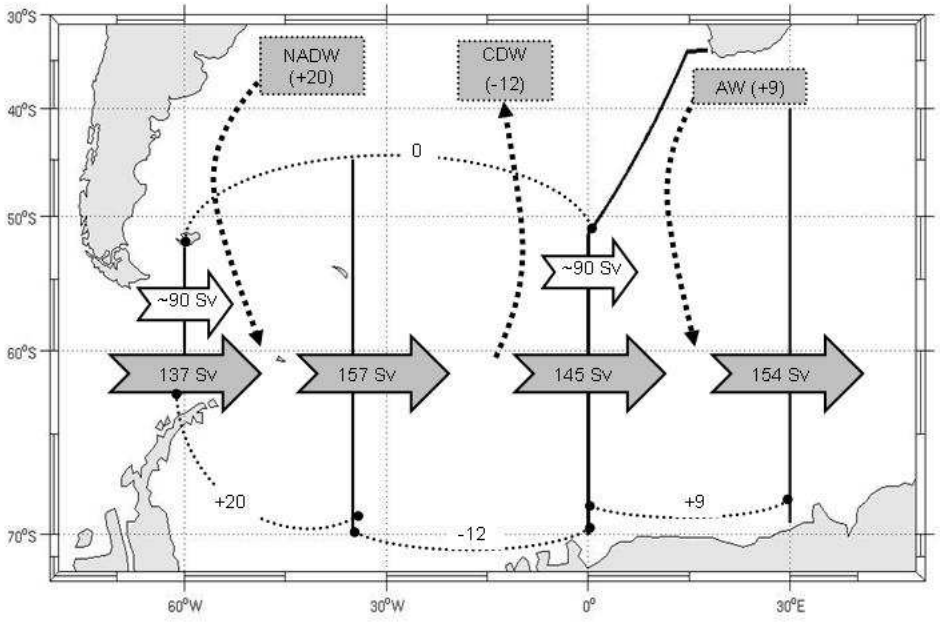

Figure 16: Schematic showing the relevant gains and loses of baroclinic transport, for the ACC, across the South Atlantic basin. The white arrows indicate the baroclinic transports referenced to 2500 dbar while the grey arrows represent the baroclinic transports relative to the bottom. The acronym AW stands for Agulhas Water, NADW= North Atlantic Deep Water and CDW= Central Deep Water. Negative values indicate volume loss from the ACC while positive values indicate volume gain to the ACC. All values are in Sv.

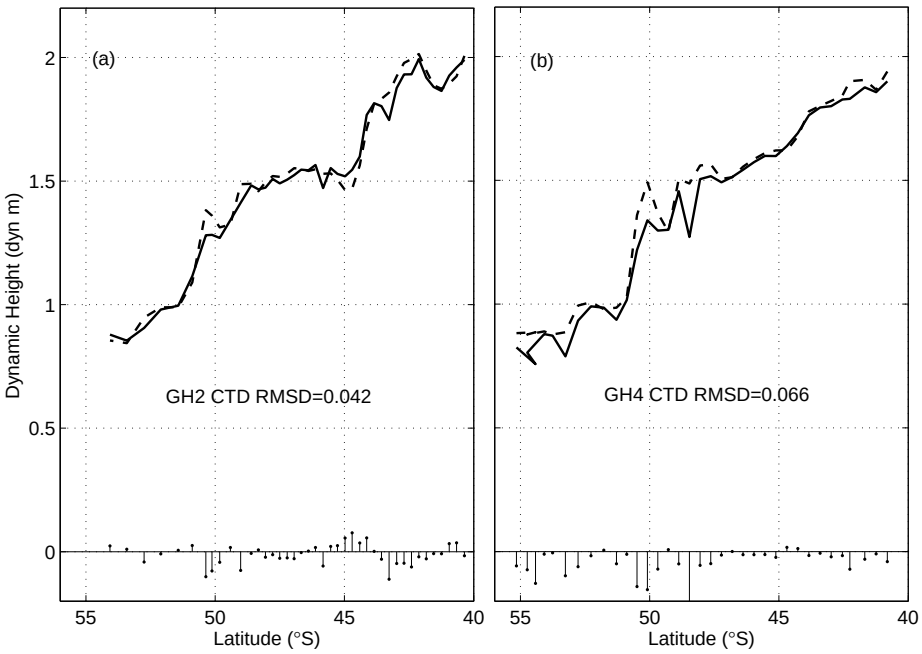

Figure 17: Comparison of surface dynamic height relative to 2500 dbar from CTD data (solid line) and from the MDH produced using altimetry data (dashed line), for two occupations of the GoodHope cruise track. The differences between the two estimates are shown along the x-axis.

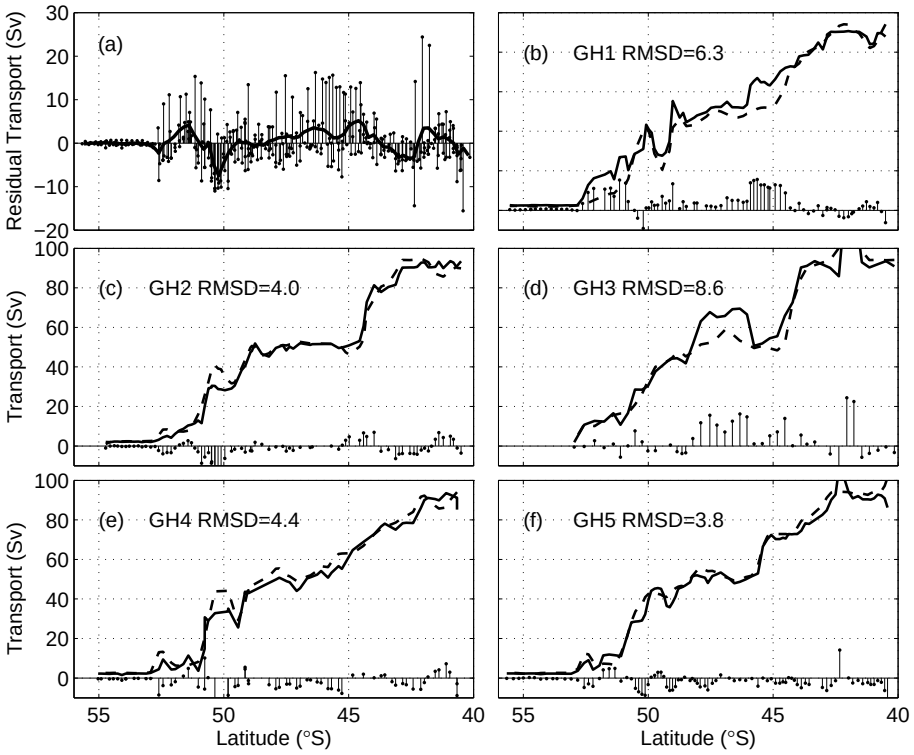

Figure 18: Comparison between baroclinic transport estimated from the MDH (dashed line) and from XBT dynamic height data (solid line; b through f), for five occupations of the GoodHope track. The difference between two transport estimates are shown along the x-axis and summarised in (a); the solid line is the mean residual plotted against latitude.

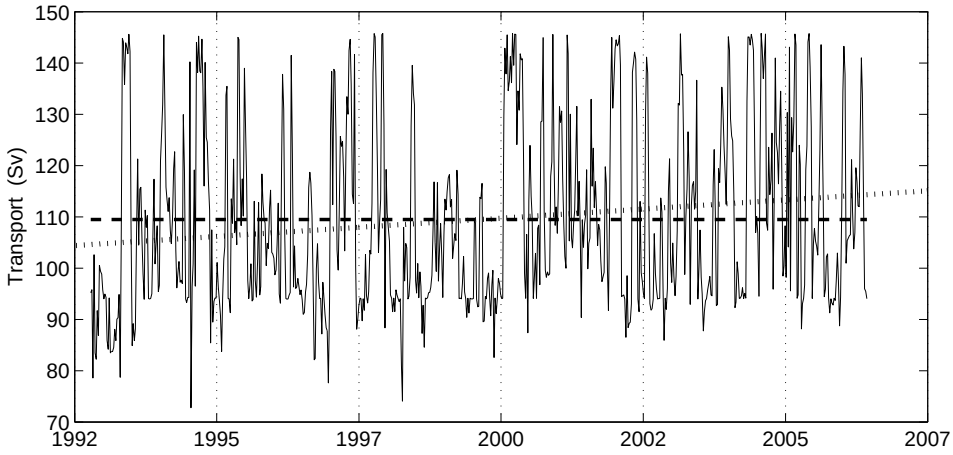

Figure 19: Time series of net baroclinic transport above 2500 dbar estimated from the MDH (solid line) between October 1992 and July 2006. The dashed line represents the mean net baroclinic transport (109.5 Sv) and the dotted line shows the linear trend applied to the data. Tick marks along the x-axis indicate start of each calendar year.